Electronic Supplementary Material (ESI) for RSC Applied Polymers.

Supporting Information

Multifunctional MXene/PAA Organohydrogel as Flexible Strain Sensor for Wearable Human-Machine Interaction

Ning Ding[a], Yan Bai[a], Yuhui Feng[a], Xiang Zou[a], Yuzhe Chen[a], Shuaihang Bi[a], Shujuan Liu[a], Weiwei Zhao[a,*], and Qiang Zhao[a,b,*]

[a.] State Key Laboratory of Organic Electronics and Information Displays & Jiangsu Key Laboratory for Biosensors, Institute of Advanced Materials (IAM), Nanjing University of Posts & Telecommunications, 9 Wenyuan Road, Nanjing 210023, China.

[b.] College of Electronic and Optical Engineering & College of Flexible Electronics (Future Technology), Nanjing University of Posts & Telecommunications, 9 Wenyuan, Nanjing 210023, China.

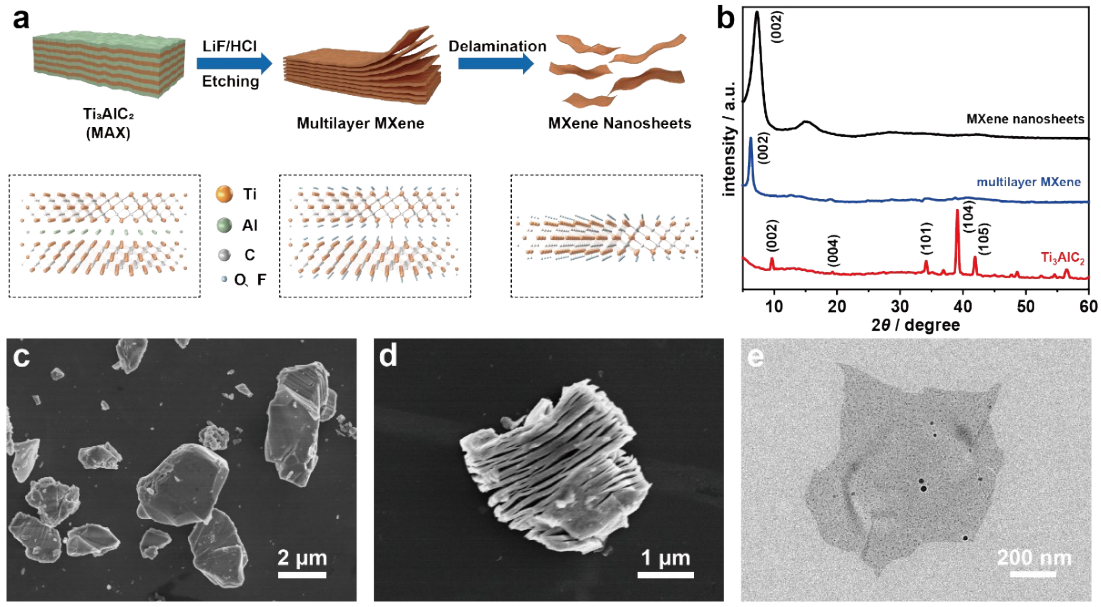

Fig. S1 a) Schematic illustration of etching MAX and stripping multilayer MXene. b) XRD patterns of Ti_3AlC_2, accordion-like multilayer MXene and MXene nanosheets. SEM images of Ti_3AlC_2 bulks c) and multilayer MXene d). e) TEM image of MXene nanosheets.

Compared to Ti_3AlC_2 bulks, the peak intensity of multilayer MXene at 39° shows a significant decrease, suggesting the successful removal of the majority of Al layers through etching. Furthermore, the shift in the (002) peak towards a smaller angle indicates an expansion in interlayer spacing. Notably, the peak of MXene nanosheets at 39° completely disappears, confirming the successful removal of partially etched Ti_3AlC_2 bulks after ultrasonic peeling and centrifugal collection. Consequently, a pure solution of MXene nanosheets is obtained (Fig. S1b).

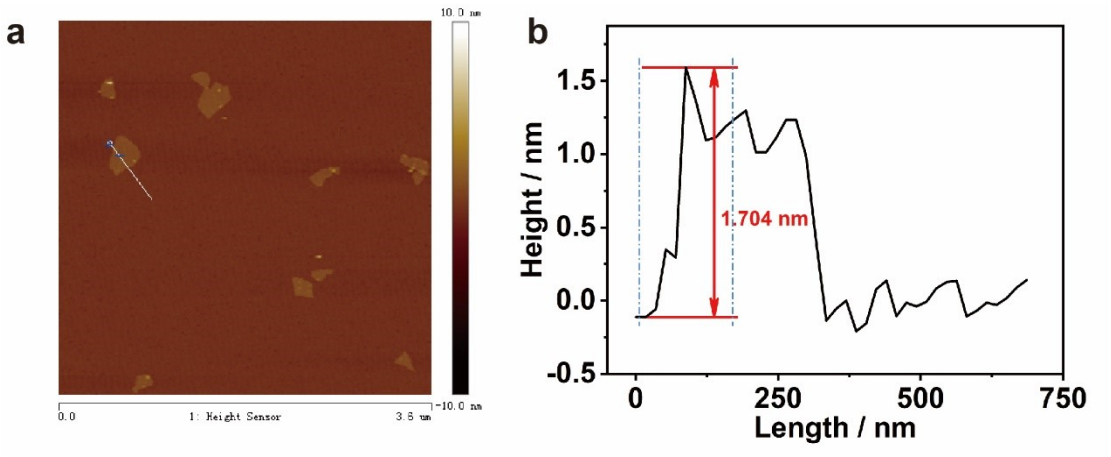

Fig. S2 AFM image a) and the corresponding thickness analysis b) of MXene nanosheets.

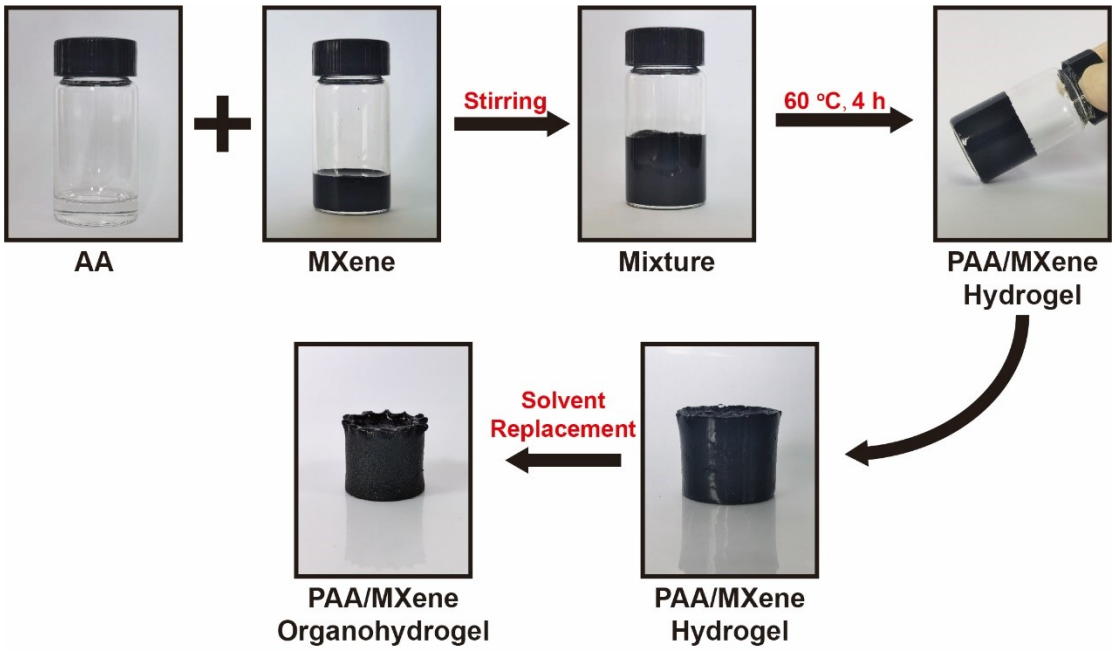

Fig. S3 Photographs of preparation process of MXene/PAA organohydrogel.

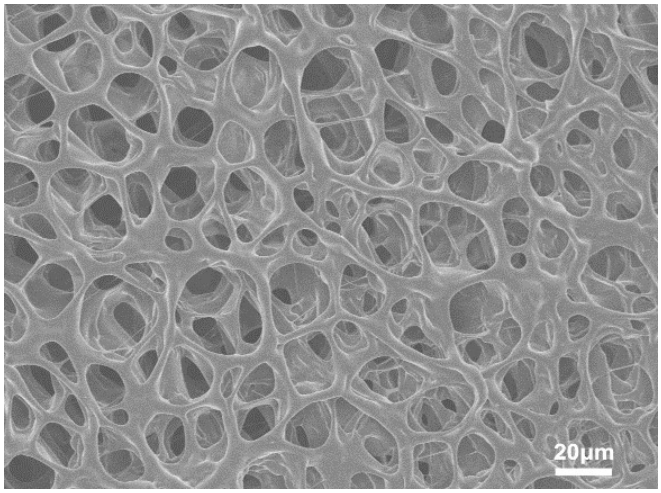

Fig. S4 SEM image of MXene/PAA hydrogel.

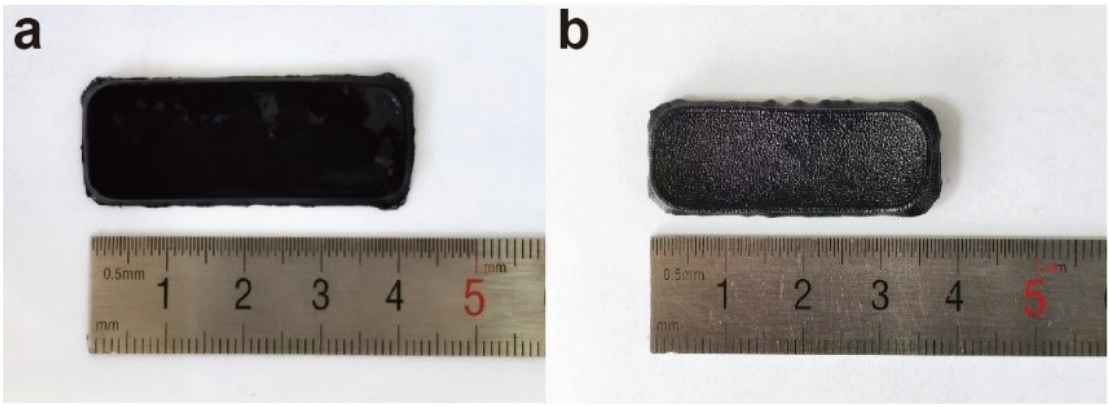

Fig. S5 Photographs of MXene/PAA hydrogel a) before and b) after solvent replacement.

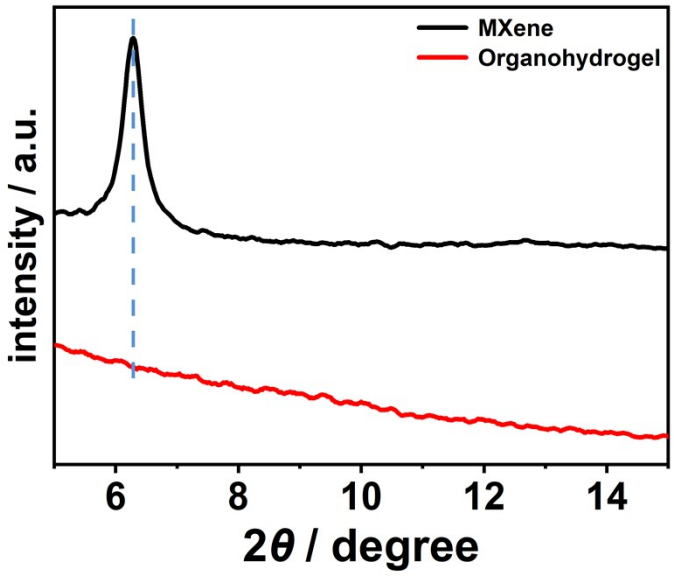

Fig. S6 XRD patterns of MXene nanosheets and MXene/PAA organohydrogel.

Compared with MXene nanosheets, XRD pattern of organohydrogel lacks obvious features or sharp diffraction peaks, indicating a lack of long-range order. This can be attributed to the complete encapsulation of MXene nanosheets during AA polymerization, resulting in their high dispersion in the organic hydrogel system.

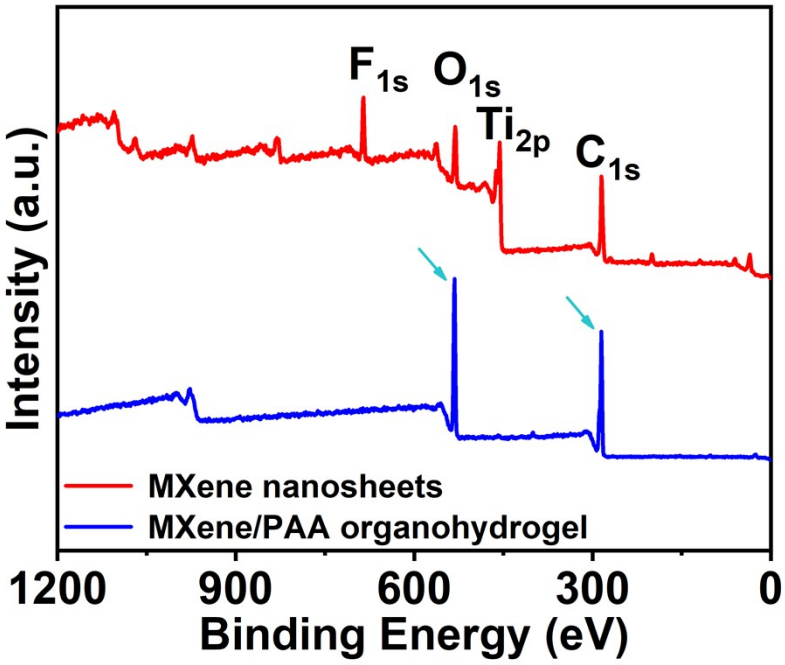

Fig. S7 XPS patterns of MXene nanosheets and MXene/PAA organohydrogel.

In comparison with pure MXene nanosheets, the peak intensity of MXene-specific elements (e.g., Ti and F) in MXene/PAA organohydrogel shows a noticeable reduction, suggesting a complete coverage and encapsulation of the MXene nanosheets by the organic polymer. The polymer molecules form a dense and continuous coating around the nanosheets, creating a physical barrier that inhibits the photoelectron escape process and attenuates the signal during XPS analysis.[1]

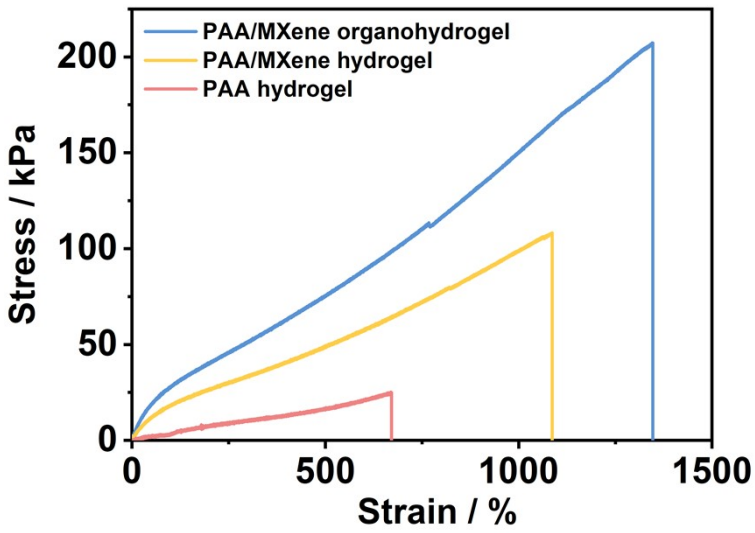

Fig. S8 Stress-strain curves of MXene/PAA organohydrogel, MXene/PAA hydrogel and PAA hydrogel.

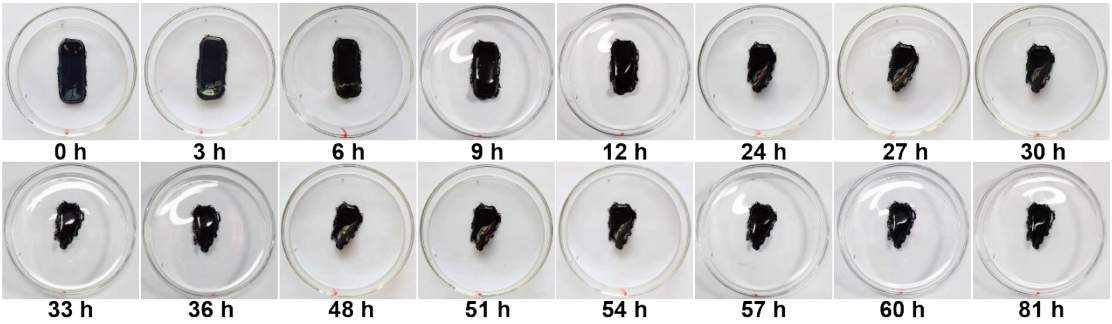

Fig. S9 Photographs of MXene/PAA hydrogel after placing for different times at 20 ^{o}C and 45% humidity.

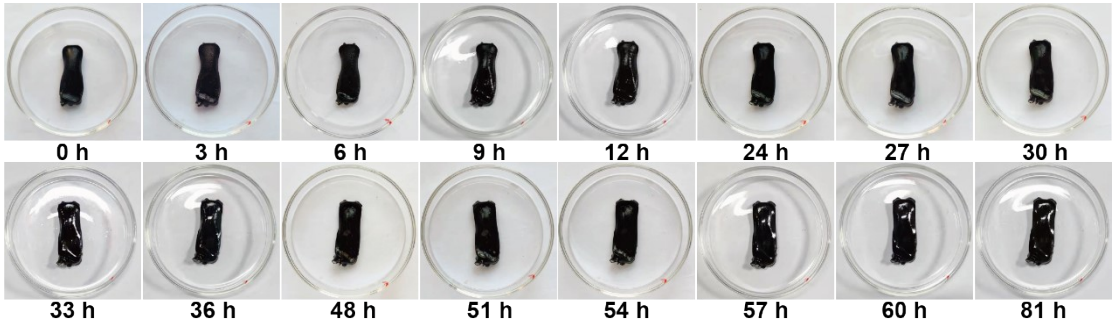

Fig. S10 Photographs of MXene/PAA organohydrogel after placing for different times at 20 ^{o}C and 45% humidity.

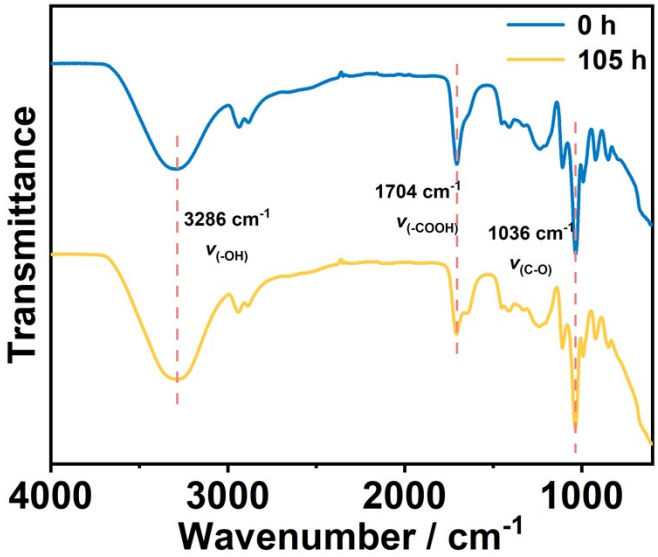

Fig. S11 ATR-FTIR spectra of MXene/PAA organohydrogel before and after placing for 105 h at 20 ^{o}C and 45% humidity.

ATR-FTIR spectra were analyzed to obtain a comprehensive understanding of the water retention capacity of MXene/PAA organohydrogel. The position of the characteristic peaks remains consistent without any noticeable shifts, indicating that the organohydrogel effectively maintains its water content for a duration of 105 hours.

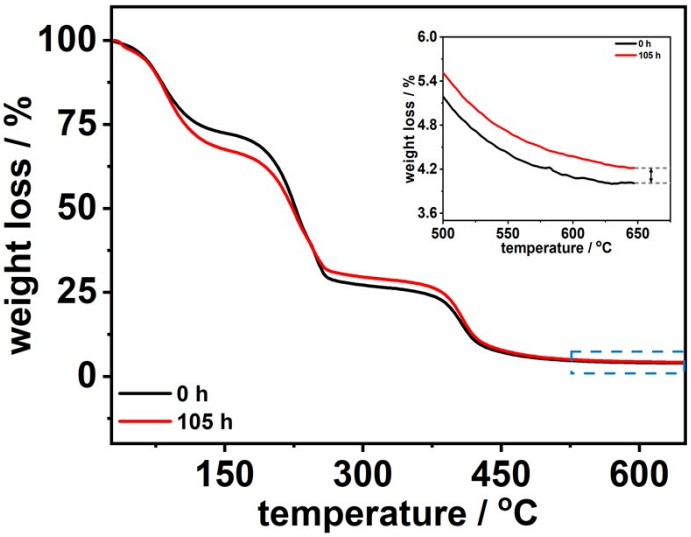

Fig. S12 TGA spectra of MXene/PAA organohydrogel before and after placing for 105 h at 20 °C and 45% humidity.

Table S1. Comparisons of the conductivity of pristine MXene, MXene/PAA hydrogel and MXene/PAA organohydrogel.

Samples	Conductivity
MXene	7241 $S \cdot cm^{-1}$
MXene/PAA hydrogel	31 $mS \cdot m^{-1}$
MXene/PAA organohydrogel	6.3 $\mu S \cdot m^{-1}$

Table S2. Comparison of comprehensive performance of different MXene-based hydrogels or organohydrogels.

gels	ε_{max} (%)	Fracture stress (MPa)	Self-healing	Adhesiveness	Anti-freezing	Moisturizing	GF	Ref.
MXene/PAA/Gly	**1346**	**0.207**	Yes	Yes	Yes	Yes	**10.96**	**This work**
MXene/PAA	1081	0.101	Yes	Yes	N/A	N/A	4.94	[2]
MXene/PVA/Borate	1200	0.0054	Yes	N/A	N/A	N/A	0.4	[3]
MXene/PVA-CA	1100	0.0097	Yes	Yes	N/A	N/A	2.3	[4]
MXene/PAA/PAM/TA	560.82	0.251	Yes	N/A	N/A	N/A	10.536	[5]
MXene/PAM/SA	2000	0.061	N/A	N/A	N/A	N/A	1.4	[6]
MXene/Gluten/EG	600	0.092	Yes	Yes	Yes	Yes	6.1	[7]
MXene/PAM/ PEDOT:PSS/EG	897	0.0293	N/A	Yes	Yes	Yes	10.69	[8]

Note: 'N/A' indicates 'not available' in the references.

Table S3. Comparison of comprehensive performance of different organohydrogels.

Organohydrogels	ε_{max} (%)	Fracture stress (MPa)	GF	Ref.
MXene/PAA/Gly	**1346**	**0.207**	**10.96**	**This work**
PG-Borate/PAM/PPy/Gly	500	0.051	4.8	[9]
PVA/CNT-OH/EG	408	0.206	1.52	[10]
PAMPs-co-PAAM/PVA/EG	648	0.075	1.77	[11]
ANF/PVA/KCl/DMSO	450	2.3	1.99	[12]
PAM/SA/TOCNs/$CaCl_2$/DMSO	681	1.04	2.1	[13]
PAA/PCA/Zn^{2+}/BDO	650	0.25	1.486	[14]

Notes and references

1 Q. Wang, X. Pan, C. Lin, H. Gao, S. Cao, Y. Ni and X. Ma, Chem. Eng. J., 2020, **401**, 126129.

2 Y. Bai, Y. Lu, S. Bi, W. Wang, F. Lin, F. Zhu, P. Yang, N. Ding, S. Liu, W. Zhao, N. Liu and Q. Zhao, Adv. Mater. Technol., 2023, **8**, 2201767.

3 J. Zhang, L. Wan, Y. Gao, X. Fang, T. Lu, L. Pan and F. Xuan, Adv. Electron., Mater. 2019, **5**, 1900285.

4 A. Chae, G. Murali, S. Y. Lee, J. Gwak, S. J. Kim, Y. J. Jeong, H. Kang, S. Park, A. S. Lee, D. Y. Koh, I. In and S. J. Park, Adv. Funct. Mater., 2023, **33**, 2213382.

5 M. Qin, W. Yuan, X. Zhang, Y. Cheng, M. Xu, Y. Wei, W. Chen and D. Huang, Colloids Surf. B, 2022, **214**, 112482.

6 H. Luan, D. Zhang, Z. Xu, W. Zhao, C. Yang and X. Chen, J. Mater. Chem. C, 2022, **10**, 7604-7613.

7 H. Xu, X. Jiang, K. Yang, J. Ren, Y. Zhai, X. Han, H. Cai and F. Gao, Colloids Surf. A Physicochem. Eng. Asp. 2022, **636**, 128182.

8 S. J. Wang, Z. Chen, X. Hu, J. Zou, Z. Xie, H. Y. Mi, Z. H. Liu, Z. Zhang, Y. Shang and X. Jing, J. Mater. Chem. C, 2022, **10**, 11914-11923.

9 Z. Bei, Y. Chen, S. Li, Z. Zhu, J. Xiong, R. He, C. Zhu, Y. Cao and Z. Qian, Chem. Eng. J., 2023, **451**, 138675.

10 W. Feng, Y. Chen, Y. Jiang, A. Hu, W. Wang and D. Yu, Polymer 2022, **262**.

11 G. Jung, H. Lee, H. Park, J. Kim, J. Wook Kim, D. Sik Kim, K. Keum, Y. Hui Lee and J. Sook Ha, Chem. Eng. J., 2022, **450**, 138379.

12 J. Lyu, Q. Zhou, H. Wang, Q. Xiao, Z. Qiang, X. Li, J. Wen, C. Ye and M. Zhu, Adv. Sci., 2023, **10**, e2206591.

13 Y. Cheng, J. Zang, X. Zhao, H. Wang and Y. Hu, Carbohydr. Polym., 2022, **277**, 118872.

14 Q. Li, J. Chen, Y. Zhang, C. Chi, G. Dong, J. Lin and Q. Chen, ACS Appl. Mater. Interfaces, 2021, **13**, 51546-51555.